

MOLECULAR DYNAMICS STUDY OF HOMOGENEOUS CRYSTAL NUCLEATION IN AMORPHOUS SILICON*

Shotaro HARA*³ Satoshi IZUMI*³ Tomohisa KUMAGAI*³ and Shinsuke SAKAI*³

*³ Department of Mechanical Engineering, University of Tokyo, 7-3-1 Hongo, Bunkyo-ku, Tokyo, Japan, 113-8656

We succeeded the simulation of homogeneous crystal nucleation in amorphous silicon by using classical molecular dynamics. The critical nucleus size was evaluated by order parameters such as potential energy, ring statistics and bond-angle deviation. We found that the size amounted to about 30-50 atoms and that shape was nearly spherical. Those results agree with the experimental data very well.

1. Introduction

Polycrystalline silicon has a number of technological applications as a thin film semiconductor. In recent years, the thickness of such a film has approached several nm and much efforts have been devoted to control the size and shape of the crystal grain, since grain geometry greatly affects the electrical and mechanical properties of thin films. From this viewpoint, crystal nucleation in the amorphous phase has been the subject of intensive experimental and theoretical study⁽¹⁾⁽²⁾. In the framework of classical nucleation theory, the size of thermodynamical critical nucleus is a key parameter to understand the nucleation process. Piriolo⁽³⁾ et al. estimated it to be 0.57 nm (40 atoms) at 953 K. Kahn⁽⁴⁾ et al. estimated it to be 0.66 nm (60 atoms) at 853 K. However, in these traditional approaches, the continuum approximation is assumed to evaluate the size of the critical nucleus because of the difficulties of the direct experimental observations for such a small nucleus. Therefore, the atomistic aspects for homogeneous nucleation are not yet fully understood.

In order to simulate the homogeneous nucleation process, the first-principle molecular dynamics is not accessible since large system size and long-time simulation are needed to achieve those simulations. Classical molecular dynamics is an effective method for

dealing with such system although the quantitative accuracy is not guaranteed. Therefore, several studies on the nucleation process, such as the condensation and evaporation process of the liquid fluid⁽⁵⁾, the droplet nucleation on the solid surface⁽⁶⁾ and the ice nucleation⁽⁷⁾, have been performed. However, as far as we know, the molecular dynamics simulation for the homogeneous nucleation in amorphous silicon has not been achieved yet. Bording et al.⁽⁸⁾ discussed the growth of the crystal grain embedded artificially in the amorphous phase. However, their evaluations are thought to be significantly affected by the initial setting of the crystal grain. Therefore, direct simulation of the nucleation is needed.

In this paper, we found the suitable conditions to realize the homogeneous nucleation simulation in the framework of the molecular dynamics. We also estimated the size and shape of the thermodynamical critical nucleus by structural analysis based on several order parameters and compared our results with those of classical nucleation theory.

2. Simulation Method

2.1 Molecular Dynamics Simulation

The Tersoff potential (T3)⁽⁹⁾ is used for an interatomic potential, which has been used in a broad range of studies of silicon and is known for its strong ability to express the physical properties of the bulk crystalline phase, the bulk amorphous phase⁽¹⁰⁾, liquid phase⁽¹¹⁾⁽¹²⁾ and surface

* 原稿受付 平成 15 年 10 月 8 日

Email: harasho@fml.t.u-tokyo.ac.jp

structure⁽¹³⁾. Especially, unlike the Stillinger-Weber (SW) potential⁽¹⁴⁾, T3 can describe the formation energy and bond length of bond defect that plays an important role in amorphization of silicon⁽¹⁵⁾.

At first, unrelaxed amorphous phase is fabricated by using melt-quench method. After melting crystal phase at 4000 K, the system is quenched to 1700 K with at a rate of 1.0×10^{14} K/sec. In order to obtain well-relaxed amorphous phases, the system is annealed for 2 ns at 1700 K. After annealing, almost all point defects such as void and interstitial have disappeared. The averaged coordination number, the ratio of the four-coordination and bond-angle deviation become 4.05, 95.1 % and 11.7° , respectively. Radial distribution function (RDF) $g(r)$ are shown in Fig. 1. Close agreement between our simulation and experimental result⁽¹⁶⁾ is shown.

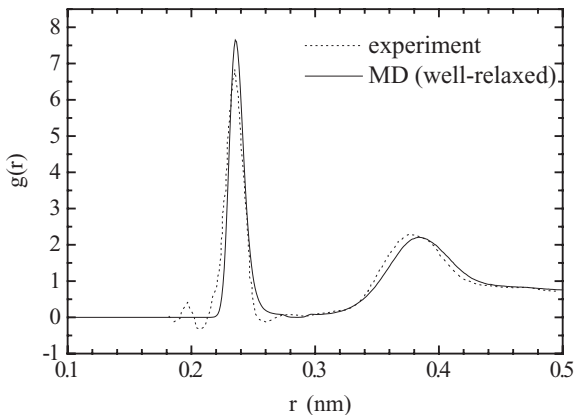


Fig. 1 Radial distribution function $g(r)$ of well-relaxed amorphous silicon obtained by molecular dynamics using the Tersoff potential (solid line). Experimental data (dotted line) is shown for comparison.

The number of atoms is 4096 and the system size is $4.42 \text{ nm} \times 4.42 \text{ nm} \times 4.42 \text{ nm}$. Periodic boundary conditions are applied to the all directions. The number of sample is 3. The well-relaxed amorphous phases are annealed for about 20 ns with the iso-volume and iso-thermal conditions. The equations of motion were integrated using the Verlet algorithm with a time step of 1.08 fs. All order parameters are averaged over 10,000 steps (10.8 ps). In experimental studies, nucleation processes are generally observed around 900 K⁽³⁾⁽⁴⁾. However, in our simulation, the homogeneous nucleation could

not be observed at 900 K. Therefore, we accelerated the nucleation processes by increasing annealing temperature. We adopted an annealing temperature of 1700 K so as not to exceed the melting points of amorphous and crystal phase. In order to estimate the melting points, we used the Brambilla method⁽¹⁷⁾ and obtained $1900 \pm 50 \text{ K}$ (amorphous) and $2350 \pm 50 \text{ K}$ (crystal). Latter value is closely similar with that obtained by Marques⁽¹⁵⁾. As is well known, the melting points of the Tersoff potential are not identical to the experimental (1420K, 1683K)⁽¹⁸⁾. Therefore, we discuss the relative temperature with respect to the melting points. To eliminate the effect of pressure on the nucleation process, the size of simulation cell was adjusted so that the stress becomes zero.

2.2 Criterion for the assignment of the atoms

When the crystal nucleus is formed in the amorphous phase, amorphous-crystal (a/c) interfaces are newly created. Since the a/c interface involves structural transition region with finite width, the assignment of the interface atoms to the amorphous and crystal phases is needed to evaluate the nucleus size.

We classify each atom into three kinds of region (crystal, amorphous and interface regions) by using order parameters. In the first step, the atoms which belong to the crystal region (crystal atoms) are detected by using bond-angle deviation $\Delta\theta$ and coordination number. At 1700 K, the atoms with the bond-angle deviation of less than 7.6° and the coordination number of exactly 4 are classified into crystal atom. In addition, the crystal atoms that bond only with non-crystal atoms are excluded. By using these criteria, we can detect the crystal atoms with the accuracy of 99.9 %.

In the second step, the atoms of the interface regions are detected step by step according to the criteria based on bond information as described below. A non-crystal atom that bonds with at least one crystal atom is classified into interface region I1. Next, a non-crystal atom that bonds with at least one atom in region I1 (previously-defined interface region) is classified into interface region I2. The second procedure is repeated until the order parameters of the newly defined interface

region coincide with those of the remaining region. Finally, the remaining atoms are classified into the amorphous region. As a result, three interface regions (I1, I2 and I3) are established. The number of interface regions depends on the broadness of the interface.

The cross-sectional view of the classification of a/c (001) interface is shown in Fig. 2, where both atoms and bonds are illustrated in the interface region and only bonds are illustrated in the crystal and amorphous regions. The interface regions are located on the transition region from ordered crystal to disordered amorphous region. That width is about 6–7 atomic layers, which amounts to 0.8–0.9 nm. The order parameters of each region are shown in Fig. 3. Smooth transitions of the order parameters are realized. That indicates our classification is well done.

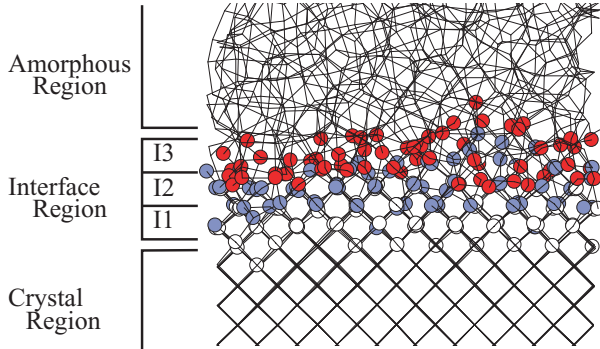


Fig. 2 Cross sectional view of the a/c (001) interface model. Both atoms and bonds are illustrated in the interface region and only bonds are illustrated in the crystal and amorphous regions.

To define the size of critical nucleus, the atoms in the interface regions must be assigned to the crystal or amorphous phases. Since this assignment includes arbitrariness, various criteria have been proposed⁽¹⁹⁾⁽²⁰⁾. We assign the atoms so that no excess volume and no excess molar number are associated with the interface. Although that scheme is based on the thermodynamics of equilibrium interfaces (Gibbsian dividing surface)⁽²¹⁾, it is frequently applied to quasi-equilibrium interfaces. In this system, this assignment is identical to the assignment in which region is divided equally between the amorphous and crystal phases, as

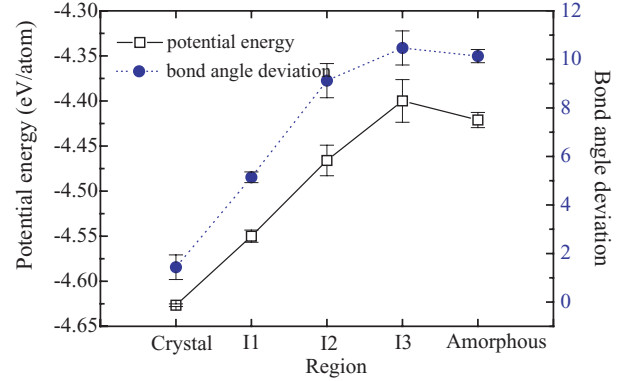


Fig. 3 Order parameters of each region. E is the potential energy per atom and $\Delta\theta$ is the bond-angle deviation.

shown in Eq. (1), where N_c and N_{int} are the number of atoms in the crystal and interface regions, respectively.

$$N_{crit} = N_c + N_{int}/2 \quad (1)$$

3. Results

3.1 Homogeneous nucleation process in amorphous silicon

Fig. 4 shows the time evolution of the potential energy E , applied pressure P and the number of crystal atoms N_c . Fig. 5 shows the snapshots of the homogeneous crystal nucleation process, where the only crystal atoms and the bonds associated with the crystal and interface atoms are illustrated.

As shown in Fig. 4, during 2–14 ns, the potential energy and pressure fluctuate around constant values. This indicates that the amorphous phase maintains the well-relaxed state. From Fig. 5, the generation and subsequent disappearance of small nuclei with a few crystal atoms are observed in various sites during 2–10 ns. After that, during 10–12 ns, the appearance and disappearance of the nucleus are repeated many times in a specific site (nucleation site). Immediately after 12 ns, the size of nucleus is thought to reach the critical value and the rapid growth of the nucleus starts. The potential energy of the whole system starts to decrease monotonically and the number of crystal

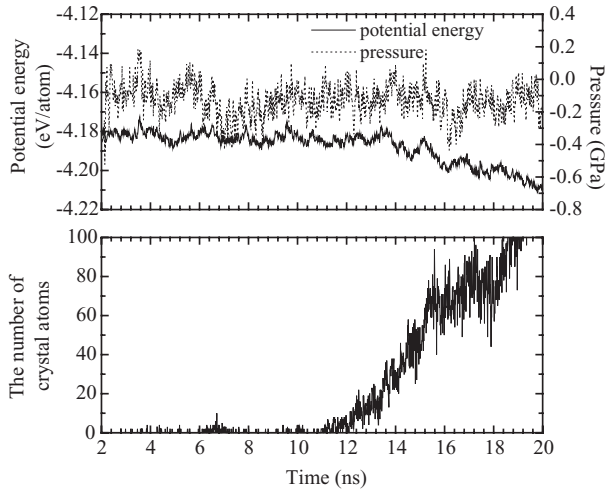


Fig. 4 Time histories of the potential energy, pressure (top), and the number of crystal atoms (bottom).

atoms start to increase drastically as shown in Fig. 4. At 15 ns, a second nucleus is generated in the same manner. The similar nucleation processes are observed in other two samples.

3.2 Quantitative evaluation of the critical size of nucleus It is difficult to detect the critical nucleus size from the order parameters of the whole system. Therefore, for the quantitative evaluation of the critical size, the detailed evaluation of the order parameters is conducted for the small cube region, which includes the nucleation site. The size of small cube is $1.4 \text{ nm} \times 1.4 \text{ nm} \times 1.4 \text{ nm}$. The cube includes 130 atoms and is referred as nucleation region hereafter. The potential energy, bond-angle deviation and the number of six-membered rings are used for the structural analysis. The time histories of the order parameters in the nucleation region are shown in Fig. 6. As a comparison, the results of the other non-nucleation region, which include the same number of atoms as that of nucleation region, are also shown.

After 5 ns, the time evolutions of the order parameters in the nucleation region deviate from those of the non-nucleation region. Those are reflected by the structural variation in the nucleation region. After the large fluctuation of the potential energy in the nucleation region at 10 ns, the number of six-membered rings dramatically increases and the potential energy gradually decreases. The

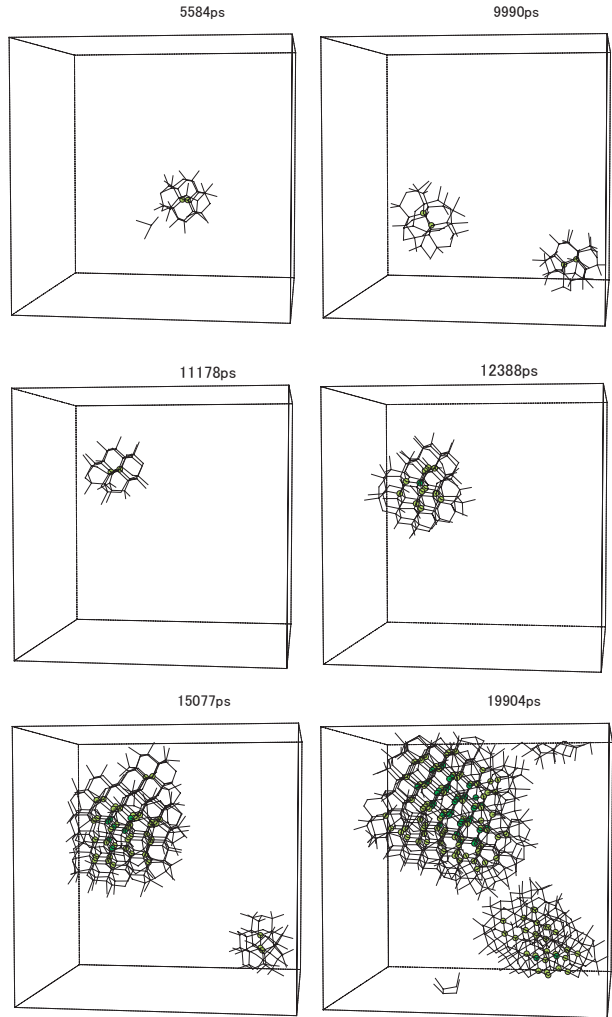


Fig. 5 Snapshots of the homogeneous nucleation process in amorphous silicon. Only crystal atoms and bonds associated with the crystal and interface atoms are illustrated.

structure of the nucleation region has completely transformed to the crystal phase and never returned to the amorphous phase after that. Fig. 7 illustrates the snapshots of the nucleation region. The appearance and disappearance of six-membered rings are observed. After 11 ns, large network of six-membered rings is formed.

Judging from the sharp increase of the number of the six-membered rings and decrease of the potential energy, we estimate the starting time of the nucleation is about 11 ns and the critical size N_{crit} is 30–50 atoms by using Eq. (1). Due to large fluctuation of the nucleus size, it is difficult to estimate it without finite scattering. As for other two samples, the same sizes of critical nucleus

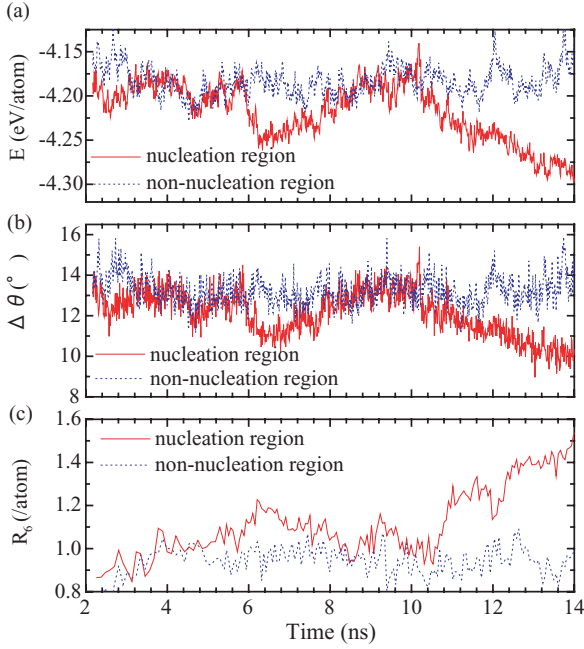


Fig. 6 Time histories of order parameters in the nucleation region and non-nucleation region: (a) potential energy per atom, E , (b) bond-angle deviation, $\Delta\theta$, (c) the number of six membered rings per atom, R_6 .

and the nucleation times of 6.5 ns and 11.5 ns are obtained. Therefore, the averaged incubation time for the homogeneous nucleation at 1700 K is about 10 ns.

Surprisingly, our result shows good agreement with the experimental value. However, we think this is accidental coincidence since other material values such as excess energy of amorphous phase with respect to crystal phase are different with experimental values. The snapshot of the nucleation region at 11.2 ns illustrated in Fig. 7 suggests that the shape of the critical nucleus is approximately spherical. This result is also supported by the weak dependence of a/c interface energy on the crystal orientation, as demonstrated in our previous work⁽²²⁾.

4. Discussions

4.1 Estimation of the critical nucleus size based on classical nucleation theory Our molecular dynamics simulations on the homogeneous nucleation estimated that the size of the crystal

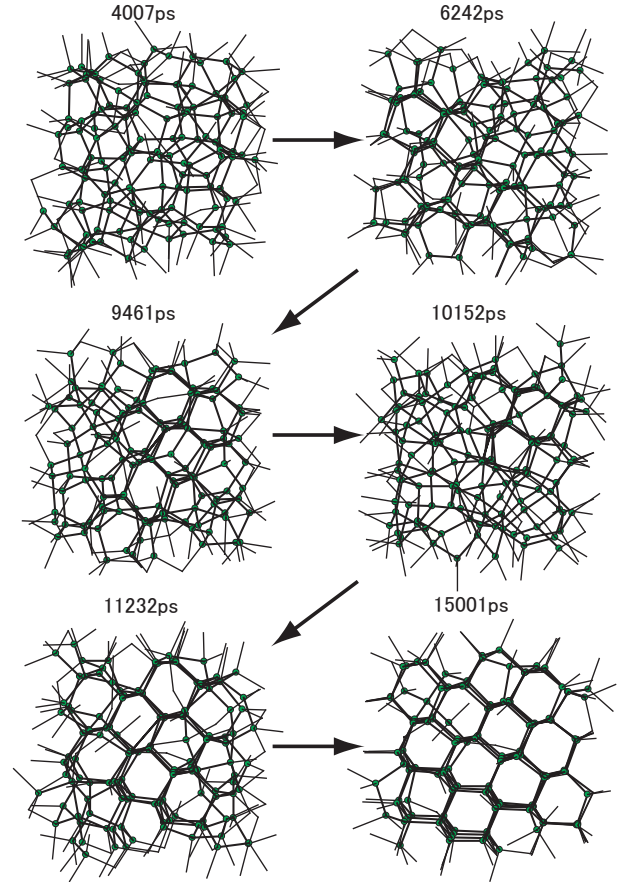


Fig. 7 Snapshots of the nucleation region. Only crystal atoms and bonds associated with the crystal and interface atoms are illustrated.

nucleus N_{crit} is about 30–50 atoms. In this section, we evaluate the critical size using the classical nucleation theory and discuss the validity of its continuum approximation. According to the classical nucleation theory, the radius of the critical nucleus (r) can be evaluated by Eq. (2), where γ is the a/c interface energy and Δg_{ac} is the excess energy of the amorphous phase with respect to the crystal phase.

$$r^* = \frac{2\gamma_{ac}}{\Delta g_{ac}} \quad (2)$$

The values of Δg_{ac} (0.17 eV/atom), $\gamma(001)$ for a/c (001) interface (0.29 J/m²) and $\gamma(111)$ for a/c (111) interface (0.33 J/m²) are obtained from the previous study⁽²²⁾, respectively. The method to detect the crystal, interface and amorphous region and to assign the interface atoms to each phase is the same as that given in this study. The contribution of the entropy term to the Δg_{ac} is approximated as about 0.03 eV from the experimental results⁽²³⁾

and the dependence of the interface energy on the temperature is neglected. Here, $\gamma = (\gamma(001) + \gamma(111))/2 = 0.31 \text{ J/m}^2$ is assumed. Consequently, the classical nucleation theory estimates the size of critical nucleus to be about 20 atoms from Eq. (2), which is slightly smaller than that estimated from our simulation. In addition to the inaccurate estimation of the values of γ and Δg_{ac} caused by the several assumptions as described above, this disagreement might be attributed to the size of the nucleus. According to the continuum approximation, homogeneous nucleuses and sharp interfaces with zero-width are assumed. However, in the case of the homogeneous nucleation in amorphous silicon, the radius of the critical nucleus r ($=0.6 \text{ nm}$) is comparable to the width of the interface region ($0.8\text{--}0.9 \text{ nm}$). In other words, it is doubtful that the continuum theory can be applied to such a small region. Therefore, a modified nucleation theory including the effect of the interface width must be developed.

4.2 Effect of simulation cell size on size of critical nucleus If the all interface atoms are included in the critical nucleus, that size reaches about 100 atoms. Therefore, in order to avoid the artificial effect of the boundary conditions, large simulation cell is needed. For the verification of the cell size, we conduct a larger-scale simulation with 10648 atoms and the cell size of $6.02 \text{ nm} \times 6.02 \text{ nm} \times 6.02 \text{ nm}$. Other conditions are not changed. As a result, the critical size of the large model is closely similar with that of the original model. Therefore, the effect of the cell size is thought to be small in our model.

5. Conclusion

Molecular dynamics simulations for the homogeneous crystal nucleation in the amorphous silicon can be realized by newly optimized conditions. We adopted high temperature (1700 K) and long-time (10 ns) annealing under zero stress condition. The critical grain size is evaluated by order parameters such as potential energy, ring statistics and coordination number. When the size of nucleus exceeds the critical size, the potential energy decreases and the number of six rings significantly increases. We es-

timate the critical size is about 30–50 atoms, which shown good agreement with the experimental results. We also found that the shape of the critical nucleus is nearly spherical, which is reflected by weak dependence of a/c interface energy on the crystal orientation.

References

- (1) F. Spaepen, *Acta mater.* **48**, 31-42 (2000).
- (2) J. A. Floro, S. J. Hearne, J. A. Hunter, P. Katuka, E. Chason, S. C. Seel, C. V. Thompson, *J. Appl. Phys.* **89**, 4886 (2001).
- (3) C. Spinella, S. Lombardo, F. Piriolo, *J. Appl. Phys.* **48**, 5383 (1998).
- (4) H. Kahn, A. He, A. Heuer, *Philos. Mag. A* **82**, 137 (2002).
- (5) K. Yasuoka, M. Matsumoto, *J. Chem. Phys.* **109**, 8451-8462 (1998).
- (6) K. Yasuoka, M. Matsumoto, *J. Chem. Phys.* **109**, 8451-8462 (1998).
- (7) M. Matsumoto, S. Saito, I. Ohmine, *Nature*. **416**, 409-413 (2002).
- (8) J. K. Bording, J. Taftø, *Phys. Rev. B* **62**, 8098 (2000).
- (9) J. Tersoff, *Phys. Rev. B* **37**, 6691 (1988).
- (10) M. Ishimaru, *J. Appl. Phys.* **91**, 686 (2002).
- (11) S. Cook, P. Clancy, *Phys. Rev. B* **47**, 7686 (1993).
- (12) M. Ishimaru, K. Yoshida, T. Motooka, *Phys. Rev. B* **54**, 7176 (1996).
- (13) G. Hadjisavvas, G. Kopidakis, P. Kelires, *Phys. Rev. B* **64**, 125413 (2001).
- (14) F. Stillinger, T. Weber, *Phys. Rev. B* **32**, 5262, (1985).
- (15) L. Marqués, L. Pelaz, J. Hernandez, J. Barbolla, G. Gilmer, *Phys. Rev. B* **64**, 045214 (2001).
- (16) K. Laaziri, S. Kycia, S. Roorda, M. Chicoine, J. L. Robertson, J. Wang, S. C. Moss, *Phys. Rev. B* **60**, 13520 (1999).
- (17) L. Brambilla, L. Colombo, V. Rosato, F. Cleri, *Appl. Phys. Lett.* **77**, 2337 (2000).
- (18) S. Roorda, W. C. Sinke, J. Poate, D. Jacobson, S. Dierker, B. Dennis, D. Eaglesham, F. Spaepen, *Phys. Rev. B* **44**, 3702 (1991).
- (19) N. Bernstein, M. Aziz, E. Kaxiras, *Phys. Rev. B* **58**, 4579 (1998).
- (20) F. Spaepen, *Acta Metall.* **26**, 1167 (1978).
- (21) F. Spaepen, *Solid State Phys.* **47**, 1 (1994).
- (22) S. Izumi, S. Hara, T. Kumagai, S. Sakai, IUTAM Symposium on Mesoscopic Dynamics of Fracture Process and Material Strength, July 06-11, 2003, Osaka, Japan.
- (23) E. P. Donovan, F. Spaepen, D. Turnbull, J. M. Poate, D. C. Jacobson, *J. Appl. Phys.* **57**, 1795 (1985).